A potentially common peptide target in secreted heat shock protein-90α for hypoxia-inducible factor-1α–positive tumors

Divya Sahu[a,*], Zhengwei Zhao[a,b,*], Fred Tsen[a], Chieh-Fang Cheng[a], Ryan Park[c], Alan J. Situ[d], Jinyao Dai[a], Ariana Eginli[a], Sharmineh Shams[a], Mei Chen[a], Tobias S. Ulmer[d], Peter Conti[c], David T. Woodley[a], and Wei Li[a]

[a]Department of Dermatology, University of Southern California Keck School of Medicine, Los Angeles, CA 90033; [b]State Key Laboratory of Cancer Biology, Department of Gastrointestinal Surgery, Xijing Hospital of Digestive Diseases, Fourth Military Medical University, Xian 91003, China; [c]Department of Radiation Oncology and the Norris Comprehensive Cancer Center, University of Southern California Keck School of Medicine, Los Angeles, CA 90033; [d]Department of Biochemistry and Molecular Biology and Zilkha Neurogenetic Institute, University of Southern California Keck School of Medicine, Los Angeles, CA 90033

ABSTRACT **Deregulated accumulation of hypoxia-inducible factor-1α (HIF-1α) is a hallmark of many solid tumors. Directly targeting HIF-1α for therapeutics is challenging. Our finding that HIF-1α regulates secretion of heat shock protein-90α (Hsp90α) for cell migration raises the exciting possibility that targeting the secreted Hsp90α from HIF-1α–positive tumors has a better clinical outlook. Using the HIF-1α–positive and metastatic breast cancer cells MDA-MB-231, we show that down-regulation of the deregulated HIF-1α blocks Hsp90α secretion and invasion of the cells. Reintroducing an active, but not an inactive, HIF-1α into endogenous HIF-1α–depleted cells rescues both Hsp90α secretion and invasion. Inhibition of Hsp90α secretion, neutralization of secreted Hsp90α action, or removal of the cell surface LRP-1 receptor for secreted Hsp90α reduces the tumor cell invasion in vitro and lung colonization and tumor formation in nude mice. Furthermore, we localized the tumor-promoting effect to a 115–amino acid region in secreted Hsp90α called F-5. Supplementation with F-5 is sufficient to bypass the blockade of HIF-1α depletion and resumes invasion by the tumor cells under serum-free conditions. Because normal cells do not secrete Hsp90α in the absence of stress, drugs that target F-5 should be more effective and less toxic in treatment of HIF-1α–positive tumors in humans.**

Monitoring Editor
Kunxin Luo
University of California, Berkeley

Received: Jun 28, 2011
Revised: Nov 2, 2011
Accepted: Dec 12, 2011

INTRODUCTION

In normal cells under normoxia (~8% oxygen level in tissues), the hypoxia-inducible factor-1α (HIF-1α) protein is constantly synthesized and immediately subjected to an O_2-dependent prolyl hydroxylation. This modification then targets HIF-1α to the ubiquitination-proteasome machinery for degradation (Semenza, 2003). As a result, the overall steady-state level of HIF-1α is kept low. Under hypoxia, however, HIF-1α hydroxylation and subsequent degradation are suppressed, resulting in a rise in the HIF-1α level in the cells. The increased HIF-1α then forms a functional heterodimer with the constitutively present HIF-1β (ARNT), the master transcriptional complex, called HIF-1. HIF-1 translocates into the nucleus and regulates expression of hypoxia response element–containing genes in a p300/CBP-dependent manner (Arany *et al.*, 1996). In contrast, HIF-1α proteins are kept at a constitutive level in many tumors. This is caused by the tissue hypoxia generated by outgrowth of the rapidly proliferating tumor cells over the surrounding vascular network, creating a distance that is longer than the reach of the oxygen supply from the nearest blood circulation (Bertout *et al.*, 2008). Under constant ischemia, the tumor cells then undergo genetic changes to adapt alternative and self-supporting mechanisms for continued

This article was published online ahead of print in MBoC in Press (http://www.molbiolcell.org/cgi/doi/10.1091/mbc.E11-06-0575) on December 21, 2011.

*These authors contributed equally to this work.

The authors claim no commercial interest or conflict of interest for this study.

Address correspondence to: Wei Li (wli@usc.edu).

Abbreviations used: 17-AAG, benzoquinone ansamycin 17-allylaminogeldanamycin; CM, conditioned medium; ER, estrogen receptor; FPLC, fast liquid protein chromatography; GM, geldanamycin; HIF-1, hypoxia-inducible factor-1; Hsp90, heat shock protein-90; LRP-1, LDL receptor-related protein-1; MMP9, matrix metalloproteinase-9; shRNA, short hairpin RNA; TNBC, triple negative breast cancer.

© 2012 Sahu *et al*. This article is distributed by The American Society for Cell Biology under license from the author(s). Two months after publication it is available to the public under an Attribution–Noncommercial–Share Alike 3.0 Unported Creative Commons License (http://creativecommons.org/licenses/by-nc-sa/3.0).

"ASCB®," "The American Society for Cell Biology®," and "Molecular Biology of the Cell®" are registered trademarks of The American Society of Cell Biology.

survival, expansion, and progression until neovascularization around them is complete. Thus action of oncogenes, inhibition of tumor suppressor genes, and deactivation of the enzymes involved in HIF-1α ubiquitination and degradation could all contribute to the deregulated expression of HIF-1α in tumor cells (Majmundar *et al.*, 2010). The deregulated HIF-1α plays a crucial role in tumorigenesis in animal models. Down-regulation of deregulated HIF-1α expression or inhibition of the HIF-1α action slows tumor growth and renders the tumor more susceptible to killing by radiotherapy and chemotherapy (Majmundar *et al.*, 2010). In humans, the constitutively expressed HIF-1α is linked to large tumor size, high grade, and lymph node–negative metastasis, which make the tumor less accessible to radiotherapy and chemotherapy (Hutchison *et al.*, 2004). Therefore the constitutively expressed HIF-1α in tumor cells has become a marker to predict possible outcomes of patients with tumor metastasis. Whereas sabotaging the deregulated HIF-1α in tumor cells could in concept prevent tumor progression, directly targeting the intracellularly located HIF-1α or the enzymes that regulate HIF-1α stability is challenging (Poon *et al.*, 2009).

The human heat shock protein-90 (Hsp90) chaperone family includes four confirmed members—the cytosolic Hsp90α and Hsp90β, the endoplasmic reticulum GRP74, and the mitochondrial TRAP1, which are encoded by distinct genes (Chen *et al.*, 2005). As with the overexpression (accumulation) of HIF-1α in tumor cells, Hsp90α has also been found either quantitatively overexpressed or qualitatively overactivated in a variety of tumors (Kamal *et al.*, 2003). These "extra" or "overactive" Hsp90α proteins are believed to bind and protect the stability of oncogene products inside the cell (Welch and Feramisco, 1982; Grenert *et al.*, 1997; Neckers and Neckers, 2002). Such a seemingly higher degree of protection by Hsp90α in tumor cells than their proto-oncoprotein counterparts in surrounding normal cells has been taken as the basis for a strategy for developing anticancer drugs (Whitesell *et al.*, 1994; Trepel *et al.*, 2010). Geldanamycin (GM, or benzoquinone ansamycin) and its derivatives, which bind and block the ATP-binding and ATP hydrolysis functions of Hsp90, have been the focus of drug development for more than a decade (Neckers and Neckers, 2002). GM proved to be too toxic even in animal models (Supko *et al.*, 1995). A modified form of GM, benzoquinone ansamycin 17-allylaminogeldanamycin (17-AAG), showed promising efficacy at a dose range with tolerable toxicity in preclinical studies and has entered several phase 1 and phase 2/3 clinical trials since 1999 (Solit and Chiosis 2008; Trepel *et al.*, 2010). Several newer generations of chemically modified and less toxic GM-related drugs are being developed in ongoing clinical trials. However, the main hurdle for these drugs remains as how to selectively target the oncogene-protecting activity of Hsp90 in tumors and spare the physiological function of Hsp90 in normal cells.

The figure of 1–2% of the total cellular proteins has been widely used to describe the unusual abundance of Hsp90 protein inside most types of mammalian cells. If one takes ~7000 proteins per cell, that content of Hsp90 proteins would be 70- to 150-fold higher than that of any of other cellular proteins. Csermely *et al.* (1998) argued that, if intracellular chaperoning were the only assigned function for Hsp90, such an overproduction of a single protein in cells would not be well tolerated by evolution. They speculated that the major cellular function of Hsp90 might be another, yet-unrecognized one that would require such an abundant storage of the protein. Recent studies have discovered a surprising need for normal cells to secrete the "overstocked" Hsp90α for tissue repair (Li *et al.*, 2011) and for tumor cells to constitutively secrete Hsp90α for invasion and metastasis (Tsutsumi and Neckers 2007). Secretion of Hsp90 and/or its role in invasion and/or metastasis have been reported in more than a dozen human tumors (Li *et al.*, 2011). Kuroita *et al.* (1992) reported purification of Hsp90α from conditioned media of human hybridoma SH-76 cells. Eustace *et al.* (2004) reported Hsp90α, but not Hsp90β, in conditioned media of HT-1080 fibrosarcoma cells. Wang *et al.* (2009) reported secretion of Hsp90α by MCF-7 human breast cells. Suzuki and Kulkarni (2010) found Hsp90β secreted by MG63 osteosarcoma cells. Chen *et al.* (2010) reported secretion of Hsp90α by the colorectal cancer cell line HCT-8. Work by Trutrumi and colleagues implied secretion of Hsp90α by a variety of tumor cell lines (Tsutsumi *et al.*, 2008).

What is the relationship between HIF-1α and secretion of Hsp90? HIF-1α is a key upstream regulator of Hsp90α secretion (Li *et al.*, 2007; Woodley *et al.*, 2009). Because constitutive accumulation of HIF-1α occurs in >40% of the tumors in humans (Dales *et al.*, 2005; Poon *et al.*, 2009), the secreted Hsp90α could be a new and effective target for treatment of these HIF-1α–positive tumors. In the present study, we have tested this possibility by using the estrogen receptor (ER)–negative and aryl hydrocarbon (Ah)–nonresponsive breast cancer cell line MDA-MB-231. We proved the importance of the "HIF-1α > Hsp90α secretion" axis in control of cancer cell migration and invasion for the first time. More important, we identified a critical 115–amino acid epitope, F-5, in secreted Hsp90α that provides potentially a new therapeutic target for HIF-1α–positive breast cancers and likely beyond.

RESULTS

Constitutively expressed HIF-1α is essential for invasiveness of breast cancer cells

We wanted to identify a tumor cell line with deregulated expression of HIF-1α and use this cell model for identifying new downstream effectors of the deregulated HIF-1α essential for cell invasion in vitro and tumor formation in vivo. After screening various tumor cell lines (listed in *Materials and Methods*), we focused on the triple negative breast cancer cell line MDA-MB-231, previously isolated from pleural effusion obtained from 51-year-old patient with invasive and metastatic cancer (Cailleau *et al.*, 1974). This choice also reflected the clinical data showing that ~30% of invasive breast cancer samples are hypoxic (Dales *et al.*, 2005; Lundgren *et al.*, 2007). The untransformed human epithelial cells HBL-100 (Gaffney, 1982) were included as a control. As shown in Figure 1A, in HBL-100 cells, the HIF-1α level was undetectable under normoxia (Figure 1A, a, lane 1). A time-dependent accumulation of HIF-1α protein was detected from the cells under hypoxia (lanes 2–5). Under identical conditions (equal protein loading, side-by-side operations, and enhanced chemiluminescence [ECL] processes), however, a constitutive basal level of HIF-1α expression could be detected in MDA-MB-231 cells even under normoxia (Figure 1A, c, lane 1). Whereas hypoxic treatment of the cells caused a transient increase in HIF-1α, the level reached a plateau between 3–6 h and then declined to the basal level by 14 h (lanes 2–5 and data not shown). Although the significance of this short-term induction of HIF-1α in response to hypoxia in MDA-MB-231 cells remains to be studied, the constitutive presence of HIF-1α is consistent with the increased anti–HIF-1α antibody staining of many human breast tumor tissue specimens (Dales *et al.*, 2005; Lundgren *et al.*, 2007).

The constitutive presence of HIF-1α alone in MDA-MB-231 cells is sufficient for maintaining the cells' high motility and invasiveness even under serum-free conditions (a mimic of the hypoxic tumor environment in vivo). We used the lentiviral system FG-12 to deliver a U6 promoter–driven short hairpin RNA (shRNA) against human HIF-1α or HIF-1β into MDA-MB-231 cells. This system enables

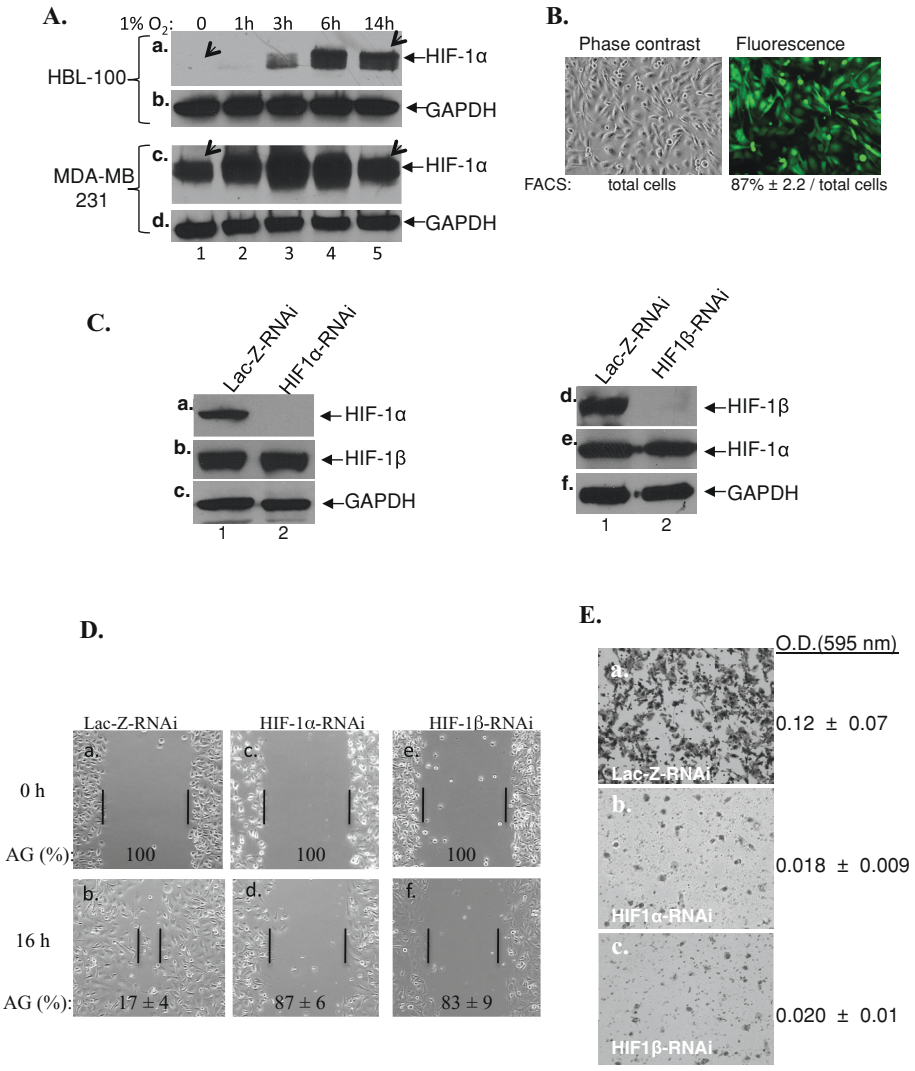

FIGURE 1: Deregulated HIF-1α is critical for breast cancer cell migration and invasion. (A) Western blot analysis of the HIF-1α levels in nontransformed breast epithelial cells (HBL-100; a, b) and breast cancer cells (MDA-MB-231; c, d) under either normoxia (21% O_2, lane 1) or hypoxia (1% O_2, lanes 2–5) over the indicated time points. Note: Equal loadings of all samples and all procedures side by side. (B) The efficiency of FG-12 lentiviral infection in MDA-MB-231 cells, as indicated by expression of an in-*cis* CMV-driven GFP gene, followed by FACS analyses. The same field was shown with either phase contrast (left) or fluorescence lens (right). (C) Specific down-regulation of HIF-1α (a) or HIF-1β (d) proteins by FG-12-delivered shRNA, as indicated by Western blot analyses. (D) Twelve-well tissue culture plates were precoated with type I collagen (20 μg/ml, 2 h). Serum-starved cells were plated (250,000 cells/well) in serum-free medium, and >90% of the cells attached within 2 h. The wound closure at 16 h was photographed and quantified as average gap (AG; Li *et al.*, 2004). n = 3, $p < 0.05$. (E) Down-regulation of HIF-1α or HIF-1β inhibited MDA-MB-231 cell invasion through a Matrigel barrier (b and c vs. a), according to manufacturer's protocol. Note: OD reading (Bio-Rad Protein Assay at 590 nm) on the penetrated cells only. The data are expressed as means ± SD (n = 4, $p < 0.05$).

>80% gene transduction efficiency in these cells, as indicated by expression of a cytomegalovirus (CMV) promoter–driven green fluorescent protein (GFP) gene in the same vector (Figure 1B, right vs. left). Under this system, as shown in Figure 1C, we achieved nearly complete down-regulation of HIF-1α (Figure 1C, a, lane 2) or HIF-1β (Figure 1C, d, lane 2), in comparison to a control shRNA against LacZ (lanes 1). Moreover, neither of the two shRNAs cross-reacted nonspecifically between HIF-1α and HIF-1β (Figure 1C, b and e). When these HIF-1α- or HIF-1β- down-regulated cells were subjected to cell motility ("scratch") assays, as shown Figure 1D, the control MDA-MB-231 cells exhibited a constitutively high motility even under serum-free conditions (Figure 1D, b vs. a). However, down-regulation of HIF-1α or HIF-1β paralyzed the cell motility (Figure 1D, d and f vs. c and e). Similar results were obtained for in vitro invasiveness of the same cells. As shown in Figure 1E, control MDA-MB-231 cells strongly penetrated a Matrigel barrier (consisting of laminin, type IV collagen, heparan sulfate proteoglycan, and nidogen) under serum-free conditions (Figure 1E, a). However, the HIF-1α– or HIF-1β–down-regulated cells exhibited a dramatic reduction in invasion (Figure 1E, b and c vs. a). These results establish the MDA-MB-231 cell line as an adequate tumor cell model to study actions of the deregulated HIF-1α.

Deregulated HIF-1α causes constitutive Hsp90α secretion

We used the following three criteria to find a key downstream and "druggable" target directly regulated by deregulated HIF-1α in MDA-MB-231 cells: 1) the protein is constitutively secreted by the cells; 2) the secretion is under direct control of the deregulated HIF-1α; and 3) function of the protein is essential for invasiveness of the tumor cells. We focused on the secreted heat shock protein-90α (Hsp90α). First, many tumor cells constitutively secrete Hsp90α (Li *et al.*, 2011). Second, hypoxia causes various types of cells to secrete Hsp90α (Li *et al.*, 2007, 2011; Woodley *et al.*, 2009). Third, secreted Hsp90α is essential for hypoxia-driven normal cell migration (Woodley *et al.*, 2009). Therefore we tested the possibility that the deregulated HIF-1α causes constitutive Hsp90α secretion, which is crucial for the invasiveness of MDA-MB-231 cells. Serum-free conditioned media (CM) of HBL-100 and MDA-MB-231 cells cultured under either normoxia or hypoxia were analyzed for the presence of Hsp90α. As shown in Figure 2A, secreted Hsp90α was detected from the CM of HBL-100 cells incubated under hypoxia (lane 2) but not normoxia (lane 1). In contrast, an equal amount of secreted Hsp90α was detected from CM of MDA-MB-231 cells cultured under either normoxia (lane 3) or hypoxia (lane 4). The constitutive secretion of Hsp90α was caused by the deregulated HIF-1α in the cells. It is shown in Figure 2B that, whereas Hsp90α secretion remained unaffected in control RNAi–infected MDA-MB-231 cells (Figure 2B, a, lane 1), secreted Hsp90α was undetectable from the CM of either HIF-1α– or HIF-1β–down-regulated MDA-MB-231 cells (Figure 2B, a, lanes 2 and 3). This inhibition appeared to be specific, since under identical conditions, secretion of matrix metalloproteinase 9 (MMP9) by the cells was rather slightly increased

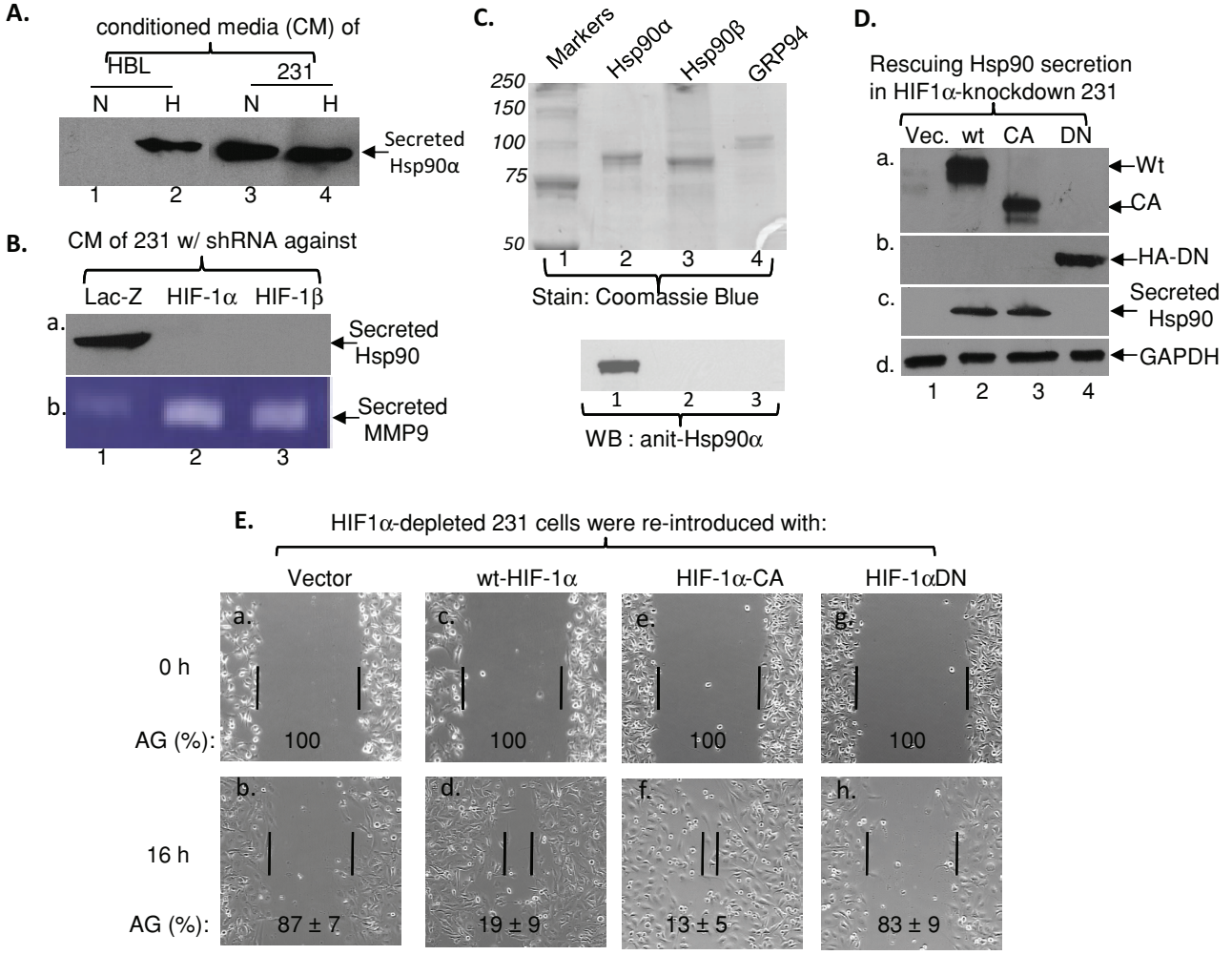

FIGURE 2: Deregulated HIF-1α uses secreted Hsp90α for migration and invasion. (A) Serum-free conditioned medium (CM; 25 μl of 10× concentrated) of HBL-100 (lanes 1 and 2) or MDA-MB-231 (lanes 3 and 4) cells incubated under normoxia (N) or hypoxia (H) for 14 h was analyzed for the presence of Hsp90α proteins by Western blotting. (B) CM of HIF-1α– or HIF-1β–down-regulated cells was analyzed for the presence of Hsp90α (a, lanes 2, 3 vs. lane 1). A 1.0-ml amount of 1× CM was concentrated 20 times and subjected to zymography gel analysis (*Materials and Methods*; b, lanes 1–3). (C) Approximately 400 ng each of recombinant Hsp90α, Hsp90β, and GRP94 were resolved on duplicate SDS gels and subjected to either Coomassie blue staining (top) or Western blot using the same anit-Hsp90α antibody (bottom). This antibody is specific against Hsp90α. (D) Reintroduction of wt and CA mutant (a, lanes 2, 3), but not dominant-negative mutant (b, lanes 4), of HIF-1α rescued Hsp90α secretion in HIF-1α–down-regulated MDA-MB-231 cells (c, lanes 2 and 3 vs. lanes 1 and 4). (E) Twelve-well tissue culture plates were coated with type I collagen (40 μg/ml, 2 h). Unattached collagens were removed by washing with Hank's balanced salt solution buffer. Serum-starved (18 h) MDA-MB-231 cells were plated (250,000 cells/well) under serum-free medium so that the cell density reached 90% confluence within 2 h. The "wounds" were made with a p-200 pipette tip. The wound closure was photographed and quantitation (AG) carried out as described (Li *et al.*, 2004). The results shown here were reproducible in three independent experiments ($n = 3$, $p < 0.05$).

(Figure 2B, b, lanes 2 and 3 vs. lane 1). Note that, unlike intracellular proteins (like β-actin or glyceraldehyde-3-phosphate dehydrogenase for intracellular protein standards), there are few reliable loading control markers for secreted proteins. The equal loadings of CM were justified by taking equal volumes of CM from the same number of cells cultured under identical conditions. Furthermore, the specificity of the anti-Hsp90α was confirmed by experiments showing that under the same conditions this antibody did not cross-react with Hsp90β or Grp94 (Figure 2C), two proteins highly related to Hsp90α.

To validate the specific control of Hsp90α secretion by HIF-1α, we carried out HIF-1α gene rescue experiments. As shown in Figure 2D, we exogenously reintroduced wild-type (wt) and constitutively active (CA) HIF-1α into endogenous HIF-1α–depleted MDA-MB-231 cells, as detected by anti–HIF-1α antibody immunoblotting analysis (Figure 2D, a, lanes 2 and 3 vs. lane 1). Because DN-HIF-1α has a large deletion that most commercial anti-HIF-1α antibodies recognize (Li *et al.*, 2007), we instead proved the expression of the 34-kDa DN-HIF-1α by using anti–hemagglutinin tag antibody blotting (Figure 2D, b, lane 4). From CM of these cells, we found that only wt-HIF-1α and CA-HIF-1α were able to rescue Hsp90α secretion (Figure 2D, c, lanes 2 and 3 vs. lane 1), but not DN-HIF-1α (lane 4). These results indicated that secreted Hsp90α is a direct downstream target for deregulated HIF-1α. More important, the wt-HIF-1α and

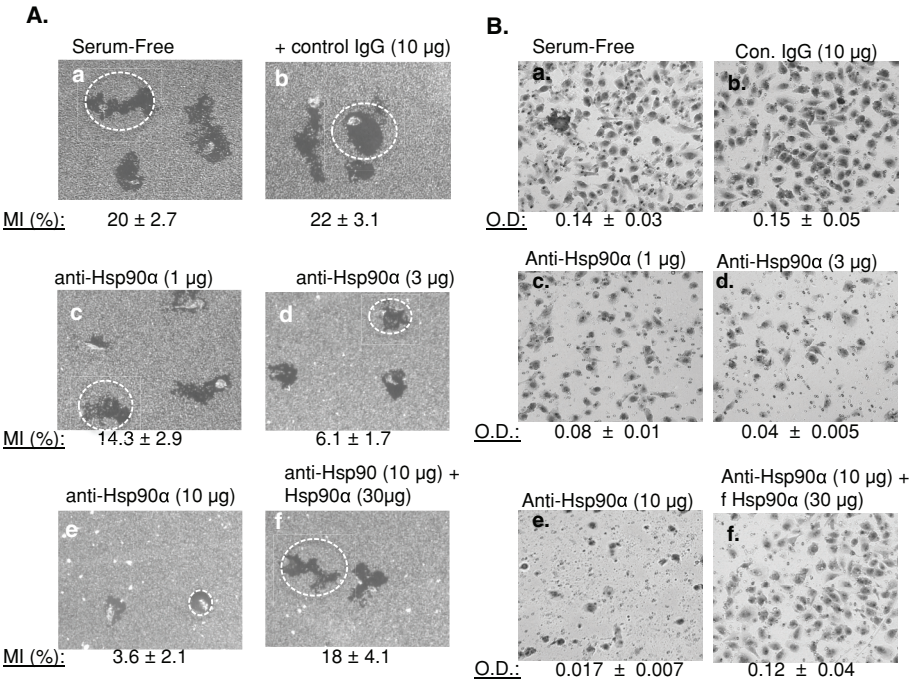

FIGURE 3: Secreted Hsp90α is essential for migration and invasion of MDA-MB-231 cells under serum-free conditions. (A) Colloidal gold migration assays show that anti-Hsp90α neutralizing antibodies blocked individual MDA-MB-231 cell motility in a dose-dependent manner (c–e vs. a, b). The addition of excess amount of recombinant Hsp90α reversed the inhibition by the antibodies (f). MI, migration index (%) (Li *et al.*, 2004). (B) Anti-Hsp90α neutralizing antibodies blocked MDA-MB-231 cell invasion through a Matrigel in a dose-dependent manner (c–e vs. a, b). The addition of excess amount of recombinant Hsp90α reversed the inhibition of invasion by the antibodies (f). The OD reading is the same as in Figure 1.

CA-HIF-1α (Figure 2E, d and f vs. b), but not DN- HIF-1α (Figure 2E, h vs. b), were also able to rescue the blocked cell motility of the endogenous HIF-1α–depleted cells (Figure 2E).

Next we examined whether secreted Hsp90α mediates deregulated HIF-1α–driven MDA-MB-231 cell migration and invasion. We used a neutralizing antibody against secreted (not intracellular) Hsp90α. We applied the colloidal gold migration assay (*Materials and Methods*), which measures individual (instead of a population) cell motility and is more relevant to Hsp90α autocrine signaling. As shown in Figure 3A, even under serum-free conditions the MDA-MB-231 cells exhibited constitutive motility (Figure 3A, a). The addition of control immunoglobulin G (IgG) showed little effect (Figure 3A, b vs. a). However, the addition of increasing amounts of the neutralizing antibody against Hsp90α into the medium inhibited the motility of the cells in a dose-dependent manner (Figure 3A, c–e). This inhibition was Hsp90α specific, since the addition of excess amounts of recombinant Hsp90α protein reversed the inhibition of cell migration by the anti-Hsp90α neutralizing antibody (Figure 3A, f). Besides its inhibitory effect on cell migration, the same neutralizing antibody also blocked the ability of MDA-MB-231 cells to invade through a Matrigel barrier. As shown in Figure 3B, the addition of increasing amounts of the antibody blocked the cell invasion in a dose-dependent manner (Figure 3B, c–e), in comparison to medium alone (Figure 3B, a) or medium with control IgG (Figure 3B, b). Similarly, the addition of excess amounts of recombinant Hsp90α protein reversed the inhibition of invasion by the anti-Hsp90α antibody (Figure 3B, f). Finally, these findings were further confirmed by a pharmacological approach. Treatment of the cells with dimethyl amiloride, a specific inhibitor of protein secretion via the exosome protein trafficking pathway (Denzer *et al.*, 2000), blocked Hsp90α secretion (Supplemental Figure S1A, lane 3 vs. lane 1) and MDA-MB-231 cell invasion in a dose-dependent manner (Figure S1B, d–f). In contrast, brefeldin A, an inhibitor of the classic endoplasmic reticulum–Golgi protein trafficking pathway (Cheng *et al.*, 2008), showed little effect on Hsp90α secretion (Figure S1A, lane 2 vs. lane 1) or cell invasion (Figure S1B, c). Taken together, the results lead us to conclude that deregulated HIF-1α in the tumor cells causes constitutive Hsp90α secretion, which is crucial for migration and invasion in the absence of any exogenous growth factors.

The percentage of Hsp90α protein in tumor versus normal cells

Although the figure of 1–2% of total cellular proteins has been widely used for decades, and half a dozen publications dating from 1984 to 2010 reported various numbers, we were unable to identify in any of those studies that a measurement had followed the required steps for estimation of a protein amount in the cells (Li *et al.*, 2011). Because we need to know how much Hsp90α each MDA-MB-231 cell has, we took textbook procedures to reestablish the percentage of Hsp90α protein in reference to total cellular proteins in four normal against four tumor cells, including the MDA-MB-231 cells. The procedures are as follows. 1) We used a series of increasing amounts of bovine serum albumin (BSA, ~55 kDa) to establish a standard curve of the actual amounts (micrograms) of BSA versus optical dichroism (OD) readings. 2) Increasing volumes of the total postnuclear extract of a given cell type were subjected to OD reading, and we converted the OD readings into micrograms of proteins according to the standard curve. 3) These cell extracts with known microgram amounts of proteins and a series of known microgram amounts of recombinant human Hsp90α protein were subjected to SDS–PAGE and Western blot with a monoclonal anti-Hsp90α antibody under exactly the same conditions. (Note: The entire processes of SDS gel electrophoresis, transferring onto nitrocellulose membranes, primary antibody blotting, secondary antibody blotting, washing, and ECL reactions of the two sets of samples were performed in common apparatus and containers and the same exposure cassette for the exactly same period of time.) 4) The Hsp90α protein bands from the cell lysates and the recombinant Hsp90α (as shown in Supplemental Figure S2) were subjected to densitometry scanning with identical parameter settings (Alpha Innotech FluorChem SP). 5) The densitometry scanning readings of the recombinant Hsp90α bands were used to establish a second standard curve that converts densitometry scanning readings to actual amounts (micrograms) of Hsp90α protein. 6) This second standard curve was used to convert the densitometry scanning readings of Hsp90α bands from the total cell extracts into micrograms of proteins. 7) Finally, the amount of Hsp90α (micrograms) in a given volume of cell extract was divided by total protein amount (micrograms) from the same cell extract times 100 to give the percentage of Hsp90α in the total proteins of the given cell type. The means of calculated numbers from eight pairs of recombinant Hsp90α versus cell extract was taken as the final percentage of Hsp90α in a given

Normal cells			Cancer cells		
Name	Origin	Percentage of Hsp90α	Name	Origin	Percentage of Hsp90α
HKC	Human keratinocyte	2.35 ± 0.26	SCC-12	Squamous carcinoma	3.29 ± 0.81
MC	Human melanocyte	2.25 ± 0.62	M-24	Human melanoma	6.76 ± 1.06
HDF	Human skin fibroblast	2.33 ± 0.16	A431	Dermal carcinoma	4.52 ± 0.70
HBL-100	Human breast epithelial	3.47 ± 0.24	MDA-MB-231	Human breast cancer	3.66 ± 0.21

The data for each cell line are the result of calculation of three independent experiments (i.e., from cell culture to densitometry). The total protein amount in cell lysate (with proteins of various molecular mass) is an estimate due to the standard curve made of a single 55-kDa protein (BSA). Based on statistical significance below $p < 0.05$, the differences between HKC vs. SCC-12 and between HBL-100 vs. MDA-MB-231 are not significant.

TABLE 1: Estimated percentage of Hsp90α in normal versus tumor cells.

cell type. As summarized in Table 1, our experiments showed that 1) Hsp90α accounts for 2–3% of the total cellular proteins in the four types of normal cells tested and it goes up to 7% of the total cellular proteins in certain tumor cell lines, and 2) Hsp90α is not elevated in all cancer cells versus their normal counterpart, such as the difference in Hsp90α between MDA-MB-231 and HBL-100 cells.

Identification of the key element in secreted Hsp90α that mediates deregulated HIF-1α–driven invasion

We used systematic mutagenesis to identify the minimum functional element in human Hsp90α. Initially, eight recombinant peptides of Hsp90α were generated and tested for stimulation of MDA-MB-231 cell motility under serum-free conditions. Five of the eight peptides (FL, F-2, F-5, F-6, and F-8), which retained various degrees of the full promotility of the full-length Hsp90α, are schematically shown in Figure 4A. The purity of the fast protein liquid chromatography (FPLC)–purified peptides was revealed by SDS–PAGE and staining (Figure 4B). F-8 is a 27–amino acid synthesized peptide (too small to show on SDS gel). Because down-regulation of the endogenous HIF-1α in MDA-MB-231 cells blocked Hsp90α secretion and reduced invasiveness of the cells, we reasoned that exogenous supplementation of functional peptides of Hsp90α should bypass the blockade of HIF-1 down-regulation and rescue the invasion defect of the cells. This rescue approach would allow us to identify the minimum functional element in secreted Hsp90α. As shown in Figure 4C, the parental and control LacZ-RNAi–infected MDA-MB-231 cells showed strong invasion (Figure 4C, a and b), whereas HIF-1α-down-regulated cells were unable to invade (Figure 4C, c). Supplementation of BSA had little effect on the invasion defect (Figure 4C, d). However, FL, F-2, and F-5 under their optimized concentrations were able to partially rescue the invasion defect of the cells (Figure 4C, e–g). In contrast, F-6 (Figure 4C, h) and F-8 (data not shown) showed significantly weaker rescuing effects, even if they still retained promotility activity. Quantitation of the data, as shown in Figure 4D, revealed that FL, F-2, and F-5 were equally effective (Figure 4D, bars e–g). F-6 was virtually unable to rescue (bar h). Similar results were obtained in HIF-1β–down-regulated MDA-MB-231 cells, in which F-5 was the shortest peptide that rescued the invasion defect of the cells (Supplemental Figure S3A). To further confirm that the rescuing mechanism by these peptides was to bypass the blockade of HIF-1α down-regulation, we found that supplementation of F-5 was unable to rescue the invasion defect of MDA-MB-231 cells with down-regulated LRP-1, the receptor for extracellular Hsp90α signaling (Cheng *et al.*, 2008; Woodley *et al.*, 2009). As shown in Figure 4E, complete down-regulation of LRP-1 by the FG-12 system (lane 2 vs. lane 1) resulted in dramatic reduction of the cell invasion (Figure 4F, b vs. a). However, the addition of F-5 was unable to rescue the LRP-1 depletion–caused invasion defect (Figure 4F, c). We also found that α-2 macroglobulin, another natural ligand for LRP-1, did not affect Hsp90α-driven MDA-MB-231 cell invasion, suggesting that these two proteins bind to distinct regions at the extracellular domain of LRP-1 (Supplemental Figure S3B).

F-5 maintains its native structure in Hsp90α

We performed CD spectroscopy to evaluate the secondary structure content of the F-5 fragment of human Hsp90α, which is highly conserved in mammals. The first half of F-5 is characterized by consecutive Glu and Lys sequence elements (Supplemental Figure S4A), which are part of the linker between the N-terminal and middle domains of human Hsp90α and which we expect to form a dynamically disordered structure. For the second half of F-5 (shown in bold), similar structural propensities as revealed in a recent crystal structure of residues 293–732 of human Hsp90 (Lee *et al.*, 2011) may be anticipated (Supplemental Figure S4B). These expectations were borne out, as shown in Supplemental Figure S4C. Approximately half of the F-5 fragment is disordered, and the detected secondary structure content correlates with the Hsp90 crystal structure, which commences with its middle domain. Thus the F-5 peptide recapitulates the structural properties of full-length Hsp90.

Interruption of Hsp90α–LRP-1 signaling in MDA-MB-231 cells blocks their ability for lung colonization and tumor formation

Colonization of various secondary organs by breast cancer depends on productive interactions between the tumor cells and the stromal microenvironment. The lung colonization assay in nude mice is an accepted model to test such ability of tumor cells. There is lack of effective and specific inhibitors against secreted Hsp90α actions in vivo. Genetic knockdown of the entire Hsp90α would not distinguish between intracellular and extracellular Hsp90α. Membrane-impermeable GM-based inhibitors were unstable and toxic to the animal when they were injected into the circulation (Tsutsumi *et al.*, 2008; Stellas *et al.*, 2010). Having considered these limitations, we took an alternative approach to target an immediate downstream effector of secreted Hsp90α, the LRP-1 receptor. We used the FG-12 system to permanently knock down LRP-1 in MDA-MB-231 cells. As shown in Figure 5A, complete down-regulation of LRP-1 was verified in the exact MDA-MB-231 cells 24 h prior to injection into nude mice (Figure 5A, a, lane 2 vs. lane 1). In addition, we found that another breast cancer cell line, MDA-MB-468, lost endogenous LRP-1 expression (Figure 5B, lane 4). Of interest, like MDA-MB-231 cells, MDA-MB-468 cells maintain constitutive HIF-1α expression and constitutive Hsp90α secretion (Figure 5C, a and c). Thus we used MDA-MB-468 cells as natural $LRP^{-/-}$ cells. All the cell lines, preengineered to stably express a luciferase gene, were injected via

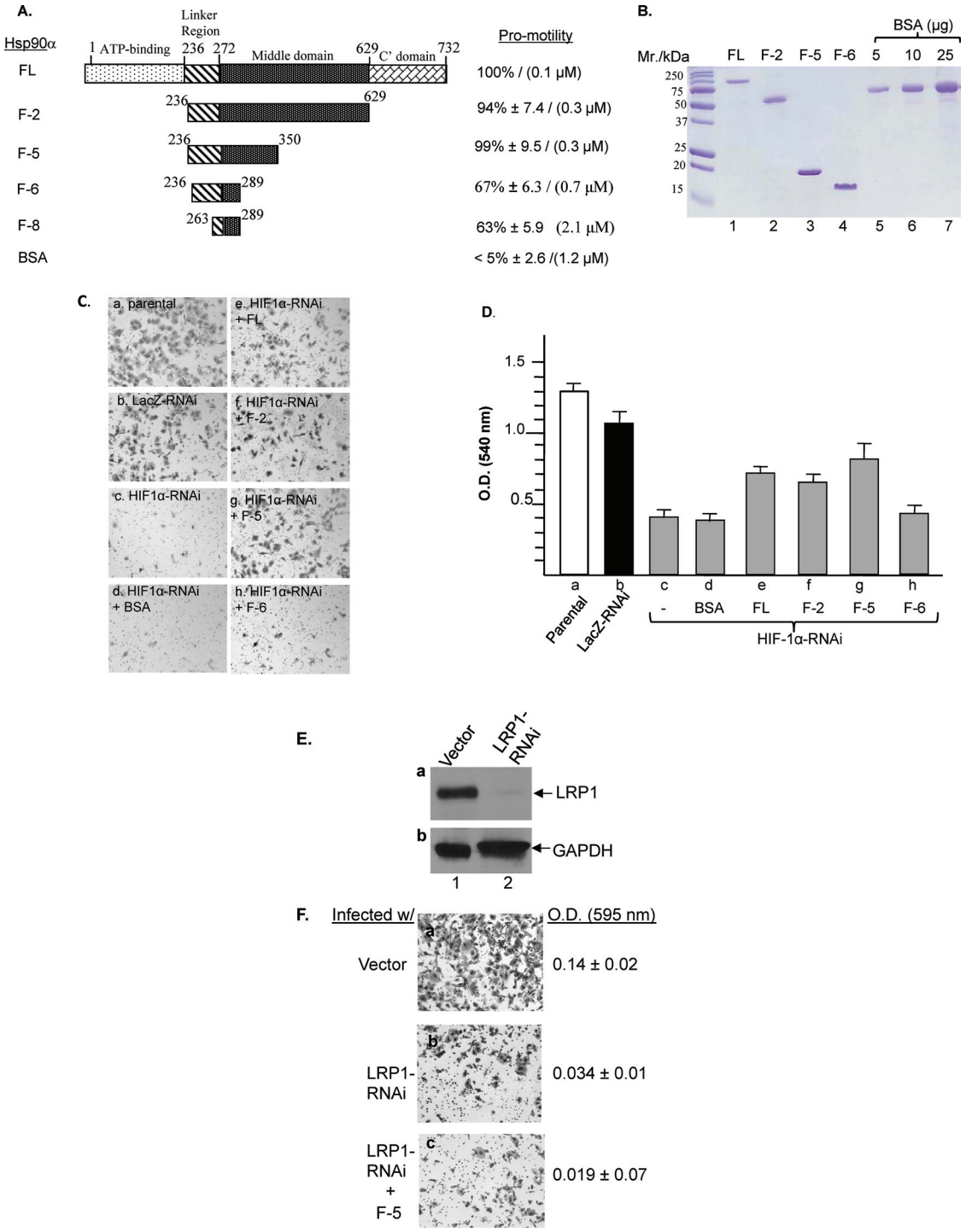

FIGURE 4: F-5 epitope in secreted Hsp90α mediates tumor cell migration and invasion. (A) A summary of truncated peptides of Hsp90α that retain either a full or partial promotility activity of full-length Hsp90α. Cell motility data are summary (%) of colloidal gold motility and "scratch" assays combined (n = 3, each assay, $p < 0.05$). (B) FPLC-purified, full-length, F-2, F-5, and F-6 were visualized in SDS gel stained with Coomassie brilliant blue (lanes 1–4), with indicated amounts of BSA as controls (lanes 5–7). F-8 is a synthetic peptide. (C) The five peptides with their optimized concentrations were tested for rescuing invasion defect of HIF-1α–down-regulated MDA-MB-231 cells. (D) Quantitation of the invasion data (n = 3, $p < 0.05$) in C. (E) Lysates of MDA-MB-231 cells infected with vector alone (lane 1) or lentivirus carrying shRNA against LRP-1 receptor (lane 2) were analyzed by Western blotting with anti–LRP-1 antibody. (F) LRP-1–down-regulated cells were unable to invade as the control cells (b vs. a), and Hsp90α was unable to rescue the invasion defect of the LRP-1–down-regulated cells (n = 4, $p < 0.05$).

tail vein into circulation of SCID mice on day 0. As shown in Figure 5D, after an initial lung homing observed for all the cell lines (1, 7, and 13), the majority of the cells became either weakly detectable or undetectable for the subsequent 4 weeks (2 and 3; 8 and 9; 14 and 15). Then the vector-infected MDA-MB-231 cells returned to develop tumors in lung around 42 d in six of seven mice per group

(Figure 5D, 4–6). In contrast, LRP-1–knockdown MDA-MB-231 cells showed much reduced ability of lung colonization (Figure 5D, 10–12), which occurred in only two out of seven mice per group. MDA-MB-468 cells showed little lung colonization in all mice. Dissection of the mice on day 70 revealed visible tumors only in lungs of the mice injected with vector MDA-MB-231, but not with LRP-1–knockdown MDA-MB-231 cells or MDA-MB-468 cells. Hematoxylin and eosin (H&E) staining of sections across the entire lung tissue, as shown in Figure 5E, showed large, invading tumors in the lungs of mice injected with vector MDA-MB-231 (Figure 5E, a and b), smaller and fewer tumors in lungs of mice injected with LRP-1–knockdown MDA-MB-231 cells (Figure 5E, c and d), and no visible tumors in lungs of mice injected with MDA-MB-468 cell (Figure 5E, e and f). Quantitation of these data is shown in Figure 5F. LRP-1 (also called CD91) is a large heterotrimeric protein consisting of a 515-kDa extracellular domain and an 85-kDa transmembrane subunit (Herz and Strickland 2001). Besides Hsp90α, several other extracellular heat shock proteins were reported to also bind LRP-1 (Basu *et al.*, 2001). Therefore the effect of LRP-1 knockdown on tumor formation did not necessarily prove that the reduced tumor formation was specifically due to blockade of secreted Hsp90α signaling through LRP-1. To address this issue, we tested whether recombinant Hsp70, gp96, and CRT, which have also been shown to bind LRP-1, promote cell migration and whether they could rescue, like Hsp90α, the invasion defect of HIF-1α–down-regulated MDA-MB-231 (Supplemental Figure S5). In both migration (Supplemental Figure S5A) and invasion (Supplemental Figure S5B) assays, Hsp70, gp96, and CRT showed limited effects. Taken together, these findings support the hypothesis that the "HIF-1 > secreted Hsp90α > LRP-1" autocrine loop plays a critical role in deregulated HIF-1α–driven tumor progression.

DISCUSSION

Under constant hypoxia, cancer cells are forced to adapt, via HIF-1α, alternative and self-supporting mechanisms for continued survival and expansion. Surface expression and secretion of Hsp90 should be constitutive in these HIF-1α–positive tumors. In fact, many types of tumor cells have recently been shown to secrete Hsp90 (Li *et al.*, 2011). Therefore targeting the secreted Hsp90 for treatment could break the boundary of tumor type and subtype specificities. Take breast cancers as an example; they are traditionally divided into three major subtypes: ER^+/PR^+, $HER2^+$ and TN (triple negative). The death rate from the disease has dropped modestly over the past decade due to the availability of multiple treatment choices: surgery, radiation, hormonal therapy, and chemotherapy. However, there remains a growing sense of frustration among breast cancer experts over side effects and unsustainable results of current treatments, such as resistance of hormone receptor–positive breast cancers to endocrine therapies. It appears that every breast cancer is genetically unique. Many of the genetic differences among individual tumors influence the likelihood that the cancer will recur (Rosman *et al.*, 2007). Dales *et al.* (2005) carried out anti–HIF-1α immunohistochemical assays on frozen sections of 745 breast cancer samples and found that the levels of HIF-1α expression correlated with poor prognosis, lower overall survival, and high metastasis risk among both node-negative and node-positive patients. By using HIF-1α expression as a marker, it was estimated that 25–40% of all invasive breast cancer samples are hypoxic, suggesting that HIF-1α can be used as a broader marker for breast cancers. In the present study, we identified a critical downstream effector of HIF-1α in breast cancer cells—the secreted Hsp90α. Of the 732–amino acid polypeptide, we narrowed down a 115–amino acid epitope called F-5 in Hsp90α that is necessary and sufficient for mediating HIF-1α–driven breast cancer cell invasion. We propose a shift of paradigm for anticancer drugs targeting Hsp90 from inhibiting the intracellular Hsp90α at its ATPase to targeting the secreted Hsp90α at the F-5 region, as schematically summarized in Figure 6.

Toxicity versus efficacy has been a long-standing challenge for anticancer drugs targeting the ATPase of intracellular Hsp90 in clinical trials. These inhibitors are expected to selectively harm the overexpressed or overly active Hsp90 in cancer cells that embed in normal tissues while minimizing potential damages in the physiological chaperone functions of Hsp90 in the surrounding normal cells and, in fact, the entire body. Difficulties in satisfying these obviously contradicting demands have prevented drug developments of this type from reaching the Food and Drug Administration as fast as they were hoped for. In contrast, as far as the secreted Hsp90α is concerned, no physiological roles (regulation of gene expression, metabolism, proliferation, and development) have been reported; instead, secretion of Hsp90α appears to be an emergency response of normal cells to tissue injury, hypoxia, or irradiation, just to mention a few. However, regardless the environmental status, tumor cells maintain a constitutive level of HIF-1α and use it to trigger Hsp90α secretion for invasion and metastasis in an otherwise nonlivable environment for normal cells (Cheng *et al.*, 2010). Therefore we propose that new anticancer drugs that selectively target the F-5 region of Hsp90α should achieve higher efficacy and pose less toxicity to cancer patients.

What are the downstream targets of secreted Hsp90α? Eustace *et al.* (2004) reported that Hsp90α, but not Hsp90β, promotes cancer cell migration and invasion by binding to and activating MMP2. Sidera *et al.* (2004, 2008) showed that a pool of cell membrane–bound Hsp90α interacts with HER-2 tyrosine kinase receptor in breast cancer cells, leading to increased MMP2 activation, cell motility, and invasion. Gopal *et al.* (2011) recently reported that extracellular Hsp90α stimulates a binding of LRP-1 to EphA2 receptor during glioblastoma cell invasion. Cheng *et al.* (2008) used four independent approaches (neutralizing antibodies, RAP inhibitor, RNAi, and somatic LRP-1–negative mutant cell line) to demonstrate that the widely expressed cell surface receptor LRP-1 mediates the extracellular Hsp90α signaling. In the present study, we show that Hsp90α failed to stimulate migration and invasion of LRP-1–down-regulated MDA-MB-231 cells in vitro. Consistently, Song *et al.* (2009) reported that LRP-1 is required for glioblastoma cell migration and invasion in vitro. Furthermore, LRP-1–down-regulated MDA-MB-231 or LRP-1–null MDA-MB-468 cells exhibited dramatically reduced lung colonization and tumor formation in vivo. Understanding how each of the target proteins contributes to Hsp90α-stimulated invasion would require simultaneous studies of these molecules in a common cell system.

Despite the various experimental approaches, direct demonstration of secreted Hsp90α in tumor progression in vivo still requires the availability of more-stable and more-specific inhibitors. Tsutsumi and colleagues used DMAG-N-oxide, a geldanamycin/17-AAG–derived and cell membrane–impermeable Hsp90 inhibitor, to pretreat melanoma cells to block extracellularly located Hsp90α, prior to injecting them into nude mice. They reported that DMAG-N-oxide–treated cells showed decreased motility and invasion of the cells in vitro and reduced lung colonization in vivo (Tsutsumi *et al.*, 2008). There are several limitations of this approach. First, 17-AAG binds and inhibits the ATPase activity of Hsp90. However, Cheng *et al.* (2008) demonstrated that the ATPase domain is dispensable for the extracellular action of Hsp90. Therefore the inhibitory effect of 17-AAG is not a direct inhibition of the functional epitope in

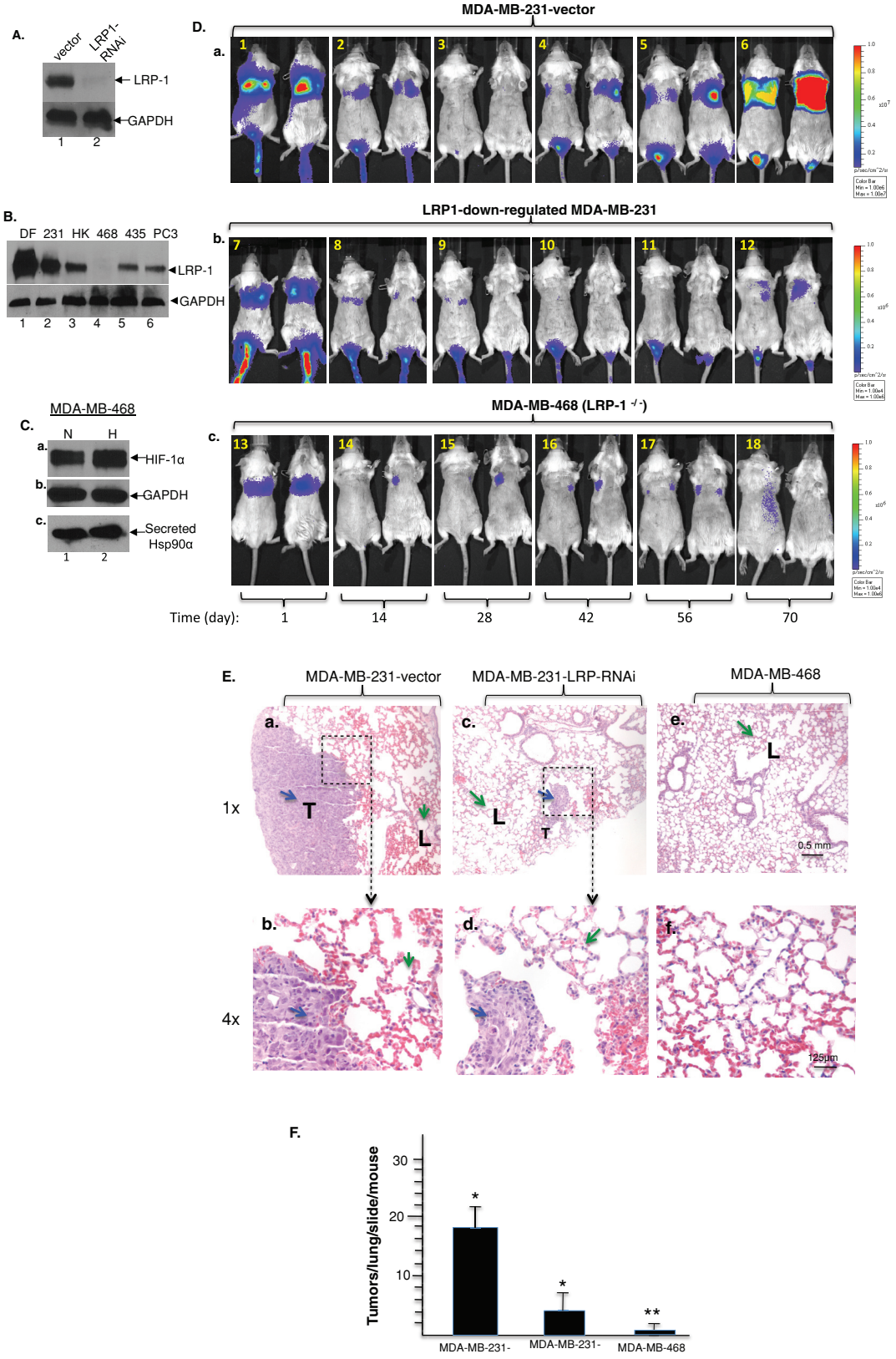

FIGURE 5: Hsp90α signaling is essential for MDA-MB-231 cell lung colonization and tumor formation in vivo. (A) Lentiviral system, FG-12, mediated shRNA-LRP-1 delivery and down-regulation of endogenous LRP-1 in MDAMB-231 cells (lane 2 vs. lane 1). (B) Western blot screening of normal and cancer cell lines for expression of LRP-1 receptor. (C) Constitutive expression of HIF-1α in MDA-MB-468 cells under either normoxia (N) or hypoxia (H; a). Constitutive secretion of Hsp90α by MDA-MB-468 cells (c). (D) Approximately 1×10^6 luciferase-engineered MDAMB-231 cells infected with either vector only (a) or vector carrying shRNA-LRP-1 (b) or LRP-$1^{-/-}$ MDAMB-468 cells (c) were injected into the tail vein of SCID mice (n = 7 per group). Whole-body bioluminescence imaging of the mice was performed once

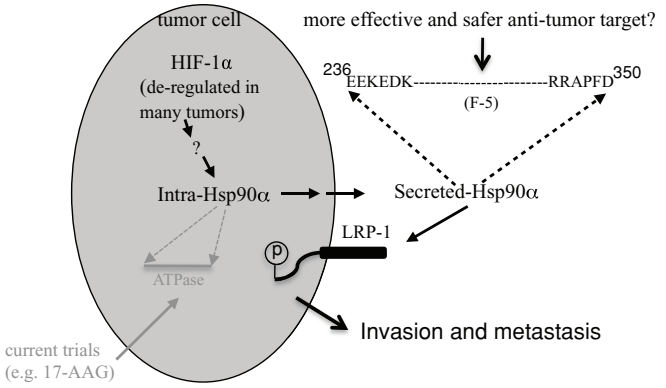

FIGURE 6: A model of secreted Hsp90α as a potential target for HIF-1α–positive cancers. The severe hypoxia often found at the center of a tumor causes constitutive accumulation of HIF-1α. The deregulated HIF-1α triggers secretion of Hsp90α via exosomes. The secreted Hsp90α binds, via F-5 epitope, to cell-surface LRP-1 receptor and promotes motility and invasion of tumor cells in an autocrine manner. Whereas current clinical trials focus on intracellular HIF-1α, we propose that targeting the F-5 epitope of secreted Hsp90α would be more effective and safer in the treatment of cancer patients.

extracellular Hsp90s. Second, it is hard to understand how a single pretreatment of the cells with the drug in vitro (due to the drug's structurally instability in vivo) could have had the reported long-lasting effect after the cells were injected into mice. Patsavoudi and colleagues reported development of a monoclonal antibody, 4C5, that neutralizes secreted Hsp90α and Hsp90β in vitro. They reported that melanoma or breast cancer cells mixed with 4C5 in vitro showed reduced lung colonization, in comparison to mixing with a control antibody, after the cells were injected into nude mice (Sidera *et al.*, 2008; Stellas *et al.*, 2010). However, it is hard to imagine that the coinjected 4C5 could have worked by continuously binding and neutralizing the constantly secreted Hsp90α and Hsp90β by the tumor cells for the entire period of the multiweek experiment. It would make more sense to inject and maintain a steady-state amount of 4C5 in circulation prior to injection with tumor cells. We showed that breast cancer cells lacking the LRP-1 receptor were unable to effectively form tumors in nude mice. As pointed out earlier, the effect of down-regulation of LRP-1 may not necessarily be due to a specific blockade of secreted Hsp90α signaling, since LRP-1 may potentially bind other, unidentified ligands. Therefore identification of the F-5 peptide in secreted Hsp90α provides an excellent target for the design of new, effective, and more-specific inhibitors for studying the role of tumor-secreted Hsp90α.

MATERIALS AND METHODS

Cell lines screened for deregulated HIF-1α expression included the following: HBl-100 human breast epithelial cell line, four human breast cancer cell lines (MDA-MB-231, MDA-MB-468, MDA-MB-435, and MCF-7), M24 and M21 human melanoma cell lines, U251 and U87 human glioma cell lines, A172 human glioblastoma cell line, PC3 human prostate cancer cell line, and A431 human skin carcinoma cell line. Native rat-tail type I collagen was from BD Biosciences (Bedford, MA). Colloidal gold (gold chloride, G4022) was purchased from Sigma-Aldrich (St. Louis, MO). The cDNAs that encode HIF-1α (wt), HIF-1αCA5 (constitutively active), and HIF-1αΔNBΔAB (dominant negative) were provided by Gregg Semenza (Johns Hopkins University, Baltimore, MD). We subcloned them into the lentiviral vector pPPLsin.MCS-Deco (Li *et al.*, 2007). ShRNAs against human HIF-1α and HIF-1β were cloned in the lentiviral FG-12 system, as previously described (Woodley *et al.*, 2009). Anti–HIF-1α antibody (610958) and anti-HIF-1β antibody (611078) were from BD Transduction Laboratories (Lexington, KY). Anti-Hsp90α antibodies for Western analysis (SPA-840) and for neutralizing function (SPS-771) were from Stressgen (Victoria, Canada). XL-10 Gold Ultra competent cells (XL-10 Gold) were from Stratagene (La Jolla, CA). The pET system (pERT15b) for protein production in *Escherichia coli* was purchased from Novagen (Madison, WI). Brefeldin A and dimethyl amiloride were purchased from Sigma-Aldrich. Matrigel invasion chambers (354480) and protocols were purchased from BD Biosciences. Athymic nude mice (4–6 wk of age; Harlan, Livermore, CA) were used in tumor formation assays.

Hypoxia treatment and preparation of serum-free conditioned media

The OxyCycler C42 from BioSpherix (Redfield, NY) was used as oxygen content controller throughout this study. This equipment allows creation of any oxygen profile with full-range oxygen (0.1–99.9%) and CO_2 control (0.1–20.0%). More important, all media used for hypoxia experiments were preincubated in hypoxia chambers with the designated oxygen content for 16 h prior to their use to replace normoxic culture media (Li *et al.*, 2007). Preparation of serum-free conditioned media was carried out as previously described (Cheng *et al.*, 2008).

Lentiviral systems for up- or down-regulation of target genes

The pRRLsinhCMV system was used to overexpress exogenous HIF-1α. The FG-12 RNAi delivery system was used to deliver shRNAs against HIF-1, as previously described (Li *et al.*, 2007; Woodley *et al.*, 2009). To measure protein levels of either endogenous or exogenous gene products, equal amounts (50 μg of total cellular proteins per sample) of cell lysate proteins (measured by Bio-Rad Protein Assay, Hercules, CA) were subjected to antibody Western blot analyses. The results were visualized by ECL reactions. Films with unsaturated exposure were used for scanning densitometry. Means from three different exposures of the same experiment were calculated (Cheng *et al.*, 2008).

Three cell migration assays and serum-free conditioned medium

Updated protocol for the colloidal gold cell motility assay, including data and statistical analysis, and a modified protocol for in vitro wound-healing assay, including precoating with an ECM, plating

a week. Representative images (two per group) of the mice show lung colonization of the injected cells at days 1, 14, 28, 56, and 70. (E) Between days 70 and 75 (note: four to five of the seven mice injected with the control MDAMB-231 cells died of tumors), mice were put to sleep and the entire lung removed and sectioned for H&E staining analyses. Blue and green arrows indicate invading tumor nodule and normal lung tissue, respectively. L, lung parenchyma; T, tumor nodule; scale bars as indicated. (F) One-way analysis of variance analysis of the staining shown in E was carried out to compare the number of tumors in the lungs of mice carrying MDA-MB-231-vector, MDA-MB-231-LRP-1RNAi, and MDA-MB-468 cells. *$p < 0.05$, **$p < 0.003$.

cells, scratching, and quantifying migration data, were as described previously (Li *et al.*, 2004). Transwell assay was performed according our previously published protocol (Li *et al.*, 2007). Preparation of serum-free conditioned medium was as described in detail previously (Cheng *et al.*, 2008). Zymography gel analysis was carried out as previously described (Zhou *et al.*, 2009).

Invasion assay

The procedures are described in detail in the manufacturer's instruction for the BD BioCoat Matrigel Invasion Chamber (354480; BD Biosciences).

Densitometry with Alpha Innotech FluorChem SP

The Alpha Innotech FluorChem SP (ProteinSimple, Santa Clara, CA) is a 4-megapixel charge-coupled device (CCD) specializing in fluorescence, chemiluminescence, or visible imaging. A 12-bit and 4–million pixel cooled camera is attached to a manual fixed lens in a MultiImage FC Light Cabinet (DE500FC) with interference filter and ML-26 dual-wavelength UV transilluminator. It uses FluorChem AlphaEase FC 32-bit software for image acquisition, enhancement, archiving, documentation, and analysis (ProteinSimple). We used 1-min exposure with an aperture set at 1.2, zoom at 20, and focus at 1.9 with an open filter and normal sensitivity and high resolution.

Recombinant Hsp90α production and purification

The coding regions of seven of the eight distinct domains (five, designated N′, M-1, M-2, C′-1, and C′-2, were as previously reported; Cheng *et al.*, 2008) were subcloned into the histidine (His)-tag pET15b vector (EMD Biosciences, San Diego, CA) at *Bam*H1 using a PCR-based cloning technique. The eighth 27–amino acid peptide, F-8, was a synthetic peptide. The pET15b-Hsp90α constructs were transformed into BL21-codonPlus (DE3)-RP competent cells (Stratagene) following the manufacturer-provided protocol. Protein synthesis was induced by the addition of 0.25 mM isopropyl-β-D-thiogalactoside (I5502-09; Sigma-Aldrich) to the bacterium culture (OD ≈ 0.8) and incubation for additional 5 h at 25°C. These His-tagged proteins were first purified by nickel-nitriloacetic acid column with the HisBind purification kit (EMD Biosciences) according to the manufacturer's procedure. The purified proteins were concentrated in Amicon Ultra (10× or 50×; Millipore, Billerica, MA) to ~4 ml, filtered (0.22 μm) prior to load onto a Superdex-200 or 75 HiLoad gel filtration column (GE Healthcare, Piscataway, NJ), and separated by FPLC. The peptides were eluted by Dulbecco's phosphate-buffered saline (DPBS) buffer (1.2 ml/min), concentrated in a Centricon YM-50 or YM-10 to 1 mg/ml, and stored in 10% glycerol–DPBS at −70°C.

Circular dichroism spectroscopy

F-5 was exchanged into 20 mM K_2HPO_4/KH_2PO_4, pH 7.4, 25 mM KCl solution by four ultrafiltration–dilution cycles (1:10 dilution) and adjusted to a concentration of 20 mM employing $e_{280\ nm}$ = 15,470 $M^{-1}\ cm^{-1}$ (Gill and Vonhippel, 1989). CD measurements were carried out at 25°C on a JASCO (Easton, MD) J-810 spectropolarimeter by acquiring spectra from 190 to 260 nm in a quartz cell of 1-cm path length. Sixteen scans, recorded in 0.1-nm steps at a rate of 50 nm/min with 0.1-nm bandwidth and 0.5-s integration time, were accumulated. Spectra were corrected for solvent contributions. The observed ellipticity in millidegrees, Q, was converted into the mean residue ellipticity, $[Q]_{MRW}$, using $[Q]_{MRW}$ = (MRW × Q)/(10dc), where d is the path length in cm, c is the protein concentration in mg/ml, and MRW (mean residue weight) is equal to MW/(n − 1), with MW denoting the molecular weight of the polypeptide chain in daltons and n representing the number of amino acids in the chain. Peptide secondary structure content was estimated using the CONTIN-LL program (Provencher and Glockner, 1981) via the DichroWeb interface (Lobley *et al.*, 2002; Whitmore and Wallace, 2004).

Tumor formation and bioluminescence imaging in mice

Athymic nude mice (4–6 wk of age; Harlan, Livermore, CA) were implanted with three different cell lines (n = 7 per cell line) to determine the role of LRP-1/CD91 signaling in lung colonization of MDAMB-231 with control shRNA (against Lac-Z), MDAMB-231 LRP-1-RNAi, and LRP-$1^{-/-}$ MDAMB-468. Mice were anesthetized with 2% isoflurane inhalant gas anesthesia using a vaporizer and injected with 1×10^6 cells/mouse intravenously via the tail vein using custom-made catheters to create the metastatic model. All animal experiments were performed in accordance with the protocol approved by the University of Southern California Institutional Animal Care and Use Committee (IACUC). Optical imaging was performed using the IVIS 200 Imaging System (Xenogen, Alameda, CA), which uses a cooled CCD camera for optimized sensitive, low-light-level in vivo imaging. Mice were anesthetized throughout the study using 2% isoflurane inhalant gas anesthesia, followed by an intraperitoneal injection of the luciferase substrate D-luciferin (50 mg/kg; Caliper Life Sciences, Alameda, CA). Distribution of the substrate occurred for 12 min, followed by bioluminescence imaging with the following settings: 1 min/scan; bin, 8; field of view, 13.1 cm; and f-stop, 1. Mice were imaged sequentially in both dorsal and ventral views during the bioluminescence signal plateau phase and analyzed using Living Image 3.1 Software (Xenogen). Mice were imaged weekly until IACUC endpoints were met. All images were normalized to the same image pseudocolor scale, and circular regions of interest were drawn over the chest area to quantify the bioluminescence signal. Data from the MDAMB-231-vector group were compared using a Wilcoxon rank-sum test for statistical significance ($p < 0.05$) and qualitatively compared with the distribution of signal from the MDAMB-231-LRP-1-RNAi and LRP-$1^{-/-}$ MDAMB-468 groups. The experiment was repeated three times.

Histochemistry

Whole lung with or without primary tumors were dissected, fixed in 10% Formalin (Sigma-Aldrich), embedded in paraffin, cut into 6-μm sections throughout the entire lung, and stained with H&E. Slides were analyzed and the tumors counted through the whole-lung section on slides using a microscope and quantified.

Statistical analyses

Cell migration and invasion data are presented as mean ± SD. All the in vitro cell experiments were analyzed with a two-tailed Student's *t* test with a confidence interval of >90%. Analysis of the lung colonization experiment data (photons/second) was performed using the two-tailed nonparametric Mann–Whitney test. $p < 0.05$ was considered statistically significant.

ACKNOWLEDGMENTS

We thank Gregg Semenza for the cDNAs of HIF-1α and HIF-1α mutants. We thank Louis Dubeau for his help in analyzing tumor sections and Jianhua Fan for her initial technical help on this project. This study was supported by National Institutes of Health Grants GM/AR67100-01 (to W.L.), AR46538 (to D.T.W.), ROIAR4798 (to M.C.), ROIAR33625 (to D.T.W. and M.C.) and Veteran Affairs Merit Award (to D.T.W.).

REFERENCES

Arany Z, Huang LE, Eckner R, Bhattacharya S, Jiang C, Goldberg MA, Bunn HF, Livingston DM (1996). An essential role for p300/CBP in the cellular response to hypoxia. Proc Natl Acad Sci USA 93, 12969–12973.

Basu S, Binder RJ, Ramalingam T, Srivastava PK (2001). CD91 is a common receptor for heat shock proteins gp96, hsp90, hsp70, and calreticulin. Immunity 14, 303–313.

Bertout JA, Patel SA, Simon MC (2008). The impact of O2 availability on human cancer. Nat Rev Cancer 8, 967–975.

Cailleau R, Young R, Olive M, Reeves WJ Jr (1974). Breast tumor cell lines from pleural effusions. J Natl Cancer Inst 53, 661–674.

Chen B, Piel WH, Gui L, Bruford E, Monteiro A (2005). The HSP90 family of genes in the human genome: insights into their divergence and evolution. Genomics 86, 627–637.

Chen JS, Hsu YM, Chen CC, Chen LL, Lee CC, Huang TS (2010). Secreted heat shock protein 90alpha induces colorectal cancer cell invasion through CD91/LRP-1 and NF-kappaB-mediated integrin alphaV expression. J Biol Chem 285, 25458–25466.

Cheng CF *et al*. (2008). Transforming growth factor alpha (TGFalpha)-stimulated secretion of HSP90alpha: using the receptor LRP-1/CD91 to promote human skin cell migration against a TGFbeta-rich environment during wound healing. Mol Cell Biol 28, 3344–3358.

Cheng CF, Fan J, Zhao Z, Woodley DT, Li W (2010). Secreted heat shock protein-90alpha: a more effective and safer target for anti-cancer drugs? Curr Signal Transduct Ther 5, 121–127.

Csermely P, Schnaider T, Soti C, Prohaszka Z, Nardai G (1998). The 90-kDa molecular chaperone family: structure, function, and clinical applications. A comprehensive review. Pharmacol Ther 79, 129–168.

Dales JP, Garcia S, Meunier-Carpentier S, Andrac-Meyer L, Haddad O, Lavaut MN, Allasia C, Bonnier P, Charpin C (2005). Overexpression of hypoxia-inducible factor HIF-1alpha predicts early relapse in breast cancer: retrospective study in a series of 745 patients. Int J Cancer 116, 734–739.

Denzer K, Kleijmeer MJ, Heijnen HF, Stoorvogel W, Geuze HJ (2000). Exosome: from internal vesicle of the multivesicular body to intercellular signaling device. J Cell Sci 113, 3365–3374.

Eustace BK *et al*. (2004). Functional proteomic screens reveal an essential extracellular role for hsp90 alpha in cancer cell invasiveness. Nat Cell Biol 6, 507–514.

Gaffney EV (1982). A cell line (HBL-100) established from human breast milk. Cell Tissue Res 227, 563–568.

Gill SC, Vonhippel PH (1989). Calculation of protein extinction coefficients from amino-acid sequence data. Anal Biochem 182, 319–326.

Gopal U, Bohonowych JE, Lema-Tome C, Liu A, Garrett-Mayer E, Wang B, Isaacs JS (2011). A novel extracellular Hsp90 mediated co-receptor function for LRP1 regulates EphA2 dependent glioblastoma cell invasion. PLoS One 8, e17649.

Grenert JP *et al*. (1997). The amino-terminal domain of heat shock protein 90 (hsp90) that binds geldanamycin is an ATP/ADP switch domain that regulates hsp90 conformation. J Biol Chem 272, 23843–23850.

Herz J, Strickland DK (2001). LRP: a multifunctional scavenger and signaling receptor. J Clin Invest 108, 779–784.

Hutchison GJ, Valentine HR, Loncaster JA, Davidson SE, Hunter RD, Roberts SA, Harris AL, Stratford IJ, Price PM, West CM (2004). Hypoxia-inducible factor 1alpha expression as an intrinsic marker of hypoxia: correlation with tumor oxygen, pimonidazole measurements, and outcome in locally advanced carcinoma of the cervix. Clin Cancer Res 10, 8405–8412.

Kamal A, Thao L, Sensintaffar J, Zhang L, Boehm MF, Fritz LC, Burrows FJ (2003). A high-affinity conformation of Hsp90 confers tumour selectivity on Hsp90 inhibitors. Nature 425, 407–410.

Kuroita T, Tachibana H, Ohashi H, Shirahata S, Murakami H (1992). Growth stimulating activity of heat shock protein 90 alpha to lymphoid cell lines in serum-free medium. Cytotechnology 8, 109–117.

Lee CC, Lin TW, Ko TP, Wang AH (2011). The hexameric structures of human heat shock protein 90. PLoS One 6, e19961.

Li W, Henry G, Fan J, Bandyopadhyay B, Pang K, Garner W, Chen M, Woodley DT (2004). Signals that initiate, augment, and provide directionality for human keratinocyte motility. J Invest Dermatol 123, 622–633.

Li W, Li Y, Guan S, Fan J, Cheng CF, Bright AM, Chinn C, Chen M, Woodley DT (2007). Extracellular heat shock protein-90alpha: linking hypoxia to skin cell motility and wound healing. EMBO J 26, 1221–1233.

Li W, Sahu D, Tsen F (2011). Secreted heat shock protein-90 (Hsp90) in wound healing and cancer. Biochim Biophys Acta Sep 25 [Epub ahead of print].

Lobley A, Whitmore L, Wallace BA (2002). DICHROWEB: an interactive website for the analysis of protein secondary structure from circular dichroism spectra. Bioinformatics 18, 211–212.

Lundgren K, Holm C, Landberg G (2007). Hypoxia and breast cancer: prognostic and therapeutic implications. Cell Mol Life Sci 64, 3233–3247.

Majmundar AJ, Wong WJ, Simon MC (2010). Hypoxia-inducible factors and the response to hypoxic stress. Mol Cell 40, 294–309.

Milani M, Harris AL (2008). Targeting tumour hypoxia in breast cancer. Eur J Cancer 44, 2766–2773.

Neckers L, Neckers K (2002). Heat-shock protein 90 inhibitors as novel cancer chemotherapeutic agents. Expert Opin Emerg Drugs 7, 277–288.

Poon E, Harris AL, Ashcroft M (2009). Targeting the hypoxia-inducible factor (HIF) pathway in cancer. Expert Rev Mol Med 11, e26.

Provencher SW, Glockner J (1981). Estimation of globular protein secondary structure from circular-dichroism. Biochemistry 20, 33–37.

Rosman DS, Kaklamani V, Pasche B (2007). New insights into breast cancer genetics and impact on patient management. Curr Treat Options Oncol 8, 61–73.

Semenza GL (2003). Targeting HIF-1 for cancer therapy. Nat Rev Cancer 3, 721–732.

Sidera K, Gaitanou M, Stellas D, Matsas R, Patsavoudi E (2008). A critical role for HSP90 in cancer cell invasion involves interaction with the extracellular domain of HER-2. J Biol Chem 283, 2031–2041.

Sidera K, Samiotaki M, Yfanti E, Panayotou G, Patsavoudi E (2004). Involvement of cell surface HSP90 in cell migration reveals a novel role in the developing nervous system. J Biol Chem 279, 45379–45388.

Solit DB, Chiosis G (2008). Development and application of Hsp90 inhibitors. Drug Discov Today 13, 38–43.

Song H, Li Y, Lee J, Schwartz AL, Bu G (2009). Low-density lipoprotein receptor-related protein 1 promotes cancer cell migration and invasion by inducing the expression of matrix metalloproteinases 2 and 9. Cancer Res 69, 879–886.

Stellas D, El Hamidieh A, Patsavoudi E (2010). Monoclonal antibody 4C5 prevents activation of MMP2 and MMP9 by disrupting their interaction with extracellular HSP90 and inhibits formation of metastatic breast cancer cell deposits. BMC Cell Bio 5, 51.

Supko JG, Hickman RL, Grever MR, Malspeis L (1995). Preclinical pharmacologic evaluation of geldanamycin as an antitumor agent. Cancer Chemother Pharmacol 36, 305–315.

Suzuki S, Kulkarni AB (2010). Extracellular heat shock protein HSP90beta secreted by MG63 osteosarcoma cells inhibits activation of latent TGF-beta1. Biochem Biophys Res Commun 39, 525–531.

Trepel J, Mollapour M, Giaccone G, Neckers L (2010). Targeting the dynamic HSP90 complex in cancer. Nat Rev Cancer 10, 537–549.

Tsutsumi S, Neckers L (2007). Extracellular heat shock protein 90: a role for a molecular chaperone in cell motility and cancer metastasis. Cancer Sci 98, 1536–1539.

Tsutsumi S, Scroggins B, Koga F, Lee MJ, Trepel J, Felts S, Carreras C, Neckers L (2008). A small molecule cell-impermeant Hsp90 antagonist inhibits tumor cell motility and invasion. Oncogene 27, 2478–2487.

Wang XX, Song W, Zhuo Y, Fu H, Shi Y, Liang M, Tong G, Chang Y Luo (2009). The regulatory mechanism of Hsp90alpha secretion and its function in tumor malignancy. Proc Natl Acad Sci USA 106, 21288–21293.

Welch WJ, Feramisco JR (1982). Purification of the major mammalian heat shock proteins. J Biol Chem 257, 14949–14959.

Whitmore L, Wallace BA (2004). DICHROWEB, an online server for protein secondary structure analyses from circular dichroism spectroscopic data. Nucleic Acids Res 32, W668–W673.

Whitesell L, Mimnaugh EG, De Costa B, Myers CE, Neckers LM (1994). Inhibition of heat shock protein HSP90-pp60v-src heteroprotein complex formation by benzoquinone ansamycins: essential role for stress proteins in oncogenic transformation. Proc Natl Acad Sci USA 91, 8324–8328.

Woodley DT, Fan J, Cheng CF, Li Y, Chen M, Bu G, Li W (2009). Participation of the lipoprotein receptor LRP1 in hypoxia-HSP90alpha autocrine signaling to promote keratinocyte migration. J Cell Sci 122, 1495–1498.

Zhou L, Yan C, Gieling RG, Kida Y, Garner W, Li W, Han YP (2009). Tumor necrosis factor-alpha induced expression of matrix metalloproteinase-9 through p21-activated kinase-1. BMC Immunol 10, 15.